DOI: 10.1002/ange.200602429

Highly Luminescent ZnO Nanocrystals Stabilized by Ionic-Liquid Components**

Da-Peng Liu, Guo-Dong Li, Yan Su, and
*Jie-Sheng Chen**

In the past two decades considerable efforts have been concentrated on the use of II–VI semiconductor nanocrystals (NCs) as luminescent materials.[1] Owing to quantum-confinement effects, the optical properties of these nanocrystals (quantum dots) can be tuned by varying the crystal size.[2] Efficient red- or green-light emitters have been prepared containing zinc (cadmium) sulfide (selenide) II–VI NCs,[3] whereas the preparation of blue-emitting NCs of these compounds has not been as successful.[4] In addition, the involvement of Cd, S, and Se in these luminescent systems may cause toxicity and pollution problems, and sulfides or selenides are intrinsically less-resistant to oxidation by the O_2 in air.

As one of the group of II–VI semiconductors, ZnO has attracted increasing attention recently because it is nontoxic, less expensive, and chemically stable towards air. However, its nanoscale crystals tend to aggregate or to undergo Ostwald ripening[5] because of their high surface energy. To stabilize NCs, appropriate surface modifications are usually necessary.[6] We have reported a facile sol–gel approach for the preparation of PEGME-modified (PEGME = poly(ethylene glycol) methyl ether) ZnO NCs with size-dependent photoluminescence (PL) and a high quantum yield (QY) of about 30% at room temperature.[7] These ZnO NCs are stable in solution, but they still undergo Ostwald ripening upon thermal treatment or aging without the protection of LiOH in the solvent-free state. Xia and co-workers recently also obtained a polymer-stabilized nano-ZnO with remarkable blue PL.[8] However, only blue-emission was observed for this luminescent system and the origin of the emission was not very clear.

Further stabilization of the NCs can be achieved if they are protected by charged species, such as alkyl ammonium cations, because the charges repel each other, thereby more effectively preventing the particles from undergoing aggregation or Ostwald ripening.[9,10] In addition, the alkyl chains of

---

[*] D. P. Liu, G. D. Li, Y. Su, Prof. J. S. Chen
State Key Laboratory of Inorganic Synthesis and Preparative Chemistry
College of Chemistry
Jilin University
Changchun 130012 (P.R. China)
Fax: (+86) 431-516-8624
E-mail: chemcj@jlu.edu.cn

[**] This work was supported by the National Natural Science Foundation of China.

Supporting Information for this article is available on the WWW under http://www.angewandte.org or from the author.

the protecting cations make the NCs more dispersible in organic solvents, which can be used to extract the NCs from the aqueous phase so as to achieve phase transfer easily.[9–11] Furthermore, upon ion-exchange with suitable counterions,[12,13] the NC-containing composite may behave as a liquid-like organic salt, usually dubbed an ionic liquid (IL) if it has a melting point below 100 °C.[14] Therefore, it is possible to enhance the processability and other physicochemical properties of NCs by modification with IL components.[12,13] Nevertheless, in all the reported work the IL-component modification was performed after the NCs were formed, and, as a result, the NC particle size and related physicochemical properties could not be tuned. Giannelis and co-workers, for example, have used positively charged organosilanes to modify the surface of ZnO NCs preformed from zinc acetate, and only a yellow-emitting (in the visible region) IL-ZnO composite with a modest QY was obtained.[13b]

Herein we describe a new approach for preparation of ZnO NCs stabilized by IL components. In this approach, the IL-ZnO nanocrystal composite is formed directly from an IL salt containing Zn^{II} cations (see Scheme 1), and the ZnO NC size, and consequently the photoluminescent properties of the NCs, can be tuned by varying the reaction conditions. The nanomaterials emit blue to yellow light efficiently both in the solvated and in the solvent-free states. Furthermore, the photoluminescent QY of the IL-ZnO materials reaches as high as 45 % in solvent, and the PL spectrum of the solvent-free IL-ZnO is stable even when the sample is heated at 80 °C.

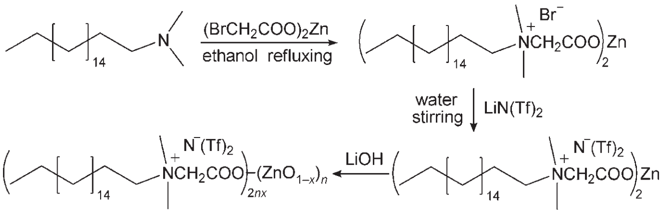

Scheme 1. Synthesis of IL-ZnO NC composites. Tf = trifluoromethanesulfonyl.

Three typical IL-ZnO samples (IL-ZnO-A, IL-ZnO-B, and IL-ZnO-C) were prepared with [LiOH]/[Zn] ratios in the reaction mixture of 3.5, 1.4, and 1.0, respectively (see Experimental Section). Figure 1 shows high-resolution transmission electron microscope (HRTEM) images of samples IL-ZnO-B and IL-ZnO-C. It can be seen that the IL-ZnO NCs are uniform and monodisperse with a diameter of about 2.5 nm for IL-ZnO-B and 4.0 nm for IL-ZnO-C; these NCs all have a wurtzite structure.[15] HRTEM images could not be obtained of the smaller IL-ZnO NCs because these composite particles always move fast under the intense electron beams.[7] IR spectroscopy indicates that the alkyl ammonium molecules are bonded to the surface of the ZnO NC cores through their carboxylate groups, and thermogravimetric and differential thermal analysis (TG-DTA) shows that the decomposition temperature of the IL-ZnO composites is above 250 °C. A calcination temperature of 600 °C results in a residue of 16.5 wt % ZnO (see Supporting Information).

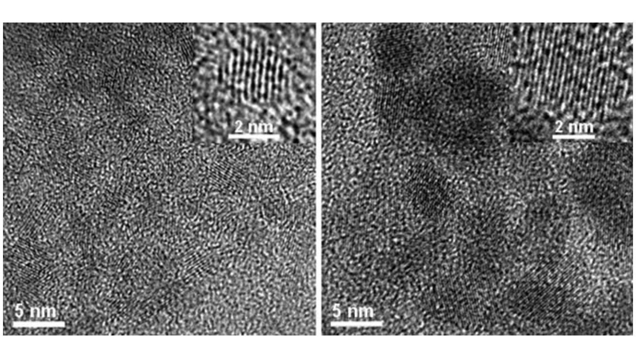

Figure 1. HRTEM images of IL-ZnO-B (left) and IL-ZnO-C (right) nanocrystals. Insets: enlarged images.

Figure 2 displays the differential scanning calorimetry (DSC) curves, which show the phase-transition process of the IL-ZnO composite. An endothermic peak appears at 33.4 °C in the heating curve (curve a) whereas an exothermic one is observed at 24.8 °C in the cooling curve (curve b). Both the heating and cooling curves show an onset of about 30 °C, which corresponds to the phase-transition temperature of the IL-ZnO system. No other phase transition is observed for the IL-ZnO sample in the temperature range of the DSC measurement.

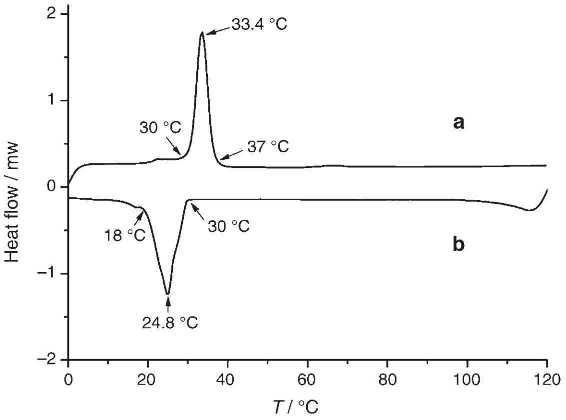

Figure 2. DSC curves for IL-ZnO-C: a) heating and b) cooling.

The PL spectra (Figure 3) show that the emission peaks of IL-ZnO-A, -B, and -C in chloroform are located at 425, 461,

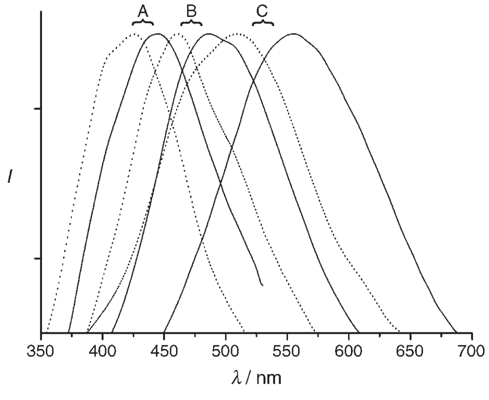

Figure 3. Normalized PL emission spectra of IL-ZnO-A, -B, and -C in the solvated state (dotted lines) and in the solvent-free state after thermal treatment at 80 °C for one week (solid lines).

and 510 nm, corresponding to purplish-blue, bluish-green, and greenish-yellow colors, respectively. The photoluminescent QYs of the materials dispersed in solvent are about 43, 45, and 41 %, respectively. After removal of the solvent under vacuum at 80 °C, the respective IL-ZnO NC samples emit blue, green, and yellow light when excited with UV radiation. Interestingly, the emission peaks of the solvent-free samples shift to 445, 495, and 555 nm, respectively (Figure 3). Nevertheless, when the solvent-free samples are re-dispersed in chloroform, the emission peaks shift back to the positions corresponding to those of the original solvated samples. This phenomenon suggests that the emission-peak shift arises from a solvent effect but not from the particle-size variation in the solvation–desolvation process. The PL spectra of the solvent-free samples remain almost unchanged after aging at 80 °C for at least one week, thus indicating that the ZnO NCs in these samples undergo no aggregation or Ostwald ripening under these conditions.

To demonstrate the light emission of the IL-ZnO NC materials further, the three solvent-free samples were each loaded in a mould with three letter-shaped grooves and illuminated with a UV lamp ($\lambda = 254$ nm). Upon UV excitation, the three letters emit blue, green, and yellow light (Figure 4, top right), respectively, in accordance with the corresponding emission spectra presented in Figure 3. Note that when the three solvent-free samples (IL-ZnO-A, -B, and -C) are mixed together in a weight ratio of approximately 1:1:1, the resulting material emits bright white light (Figure 4, middle right) with CIE (Commision Internationale de L'Eclairage) coordinates of (0.28, 0.32). This result means that by adjusting the ZnO nanocrystal size and simple mixing of the differently sized IL-ZnO NC samples, white-light emission is easily achieved. Furthermore, the IL-ZnO composite clearly shows its liquid-like features after heating. Although a phase-transition temperature of around 30 °C is observed, the composite material is still rather viscous at this temperature. However, heating to 80 °C renders the IL-ZnO sample fluid (Figure 4, bottom part). This fluidity of the IL-ZnO composite implies that the material should be highly processable upon mild thermal treatment.

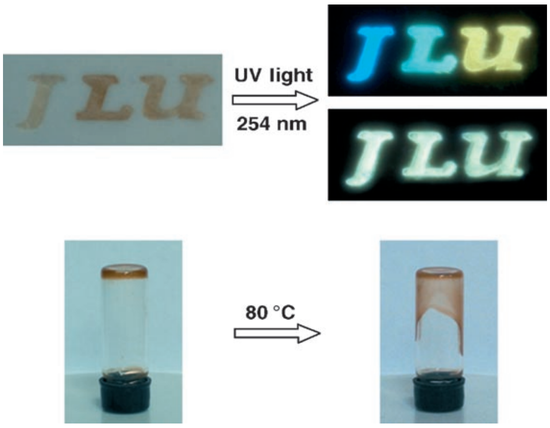

Figure 4. Photographs of IL-ZnO showing the tunable PL (upper part; see text for details) and the fluidity (lower part) of the samples.

The PL of ZnO NCs in the visible region arises from transitions involving trapped levels[15,16] and that oxygen vacancies play an important role in the formation of these trapped levels. When excited electrons in the conduction band of the NCs combine with the holes in the trapped levels, or alternatively when the electrons in the trapped levels combine with the holes in the valence band, emissions occur. The energy gaps between the conduction band and the trapped levels and those between the trapped levels and the valence band are proportional to the band gap of the NCs, therefore it is not surprising that the emission of ZnO NCs shifts to higher frequency as the NC size decreases because of quantum confinement effects. On the other hand, as the particle size of the ZnO NCs is rather small, the surface area of the NCs is distinctly larger than that of bulk ZnO crystals. This high surface area is conducive to the formation of a high concentration of oxygen vacancies, and consequently a high concentration of trapped levels in the NCs.[17] This situation explains why the photoluminescent QYs of the IL-ZnO composite materials are remarkably high. The notable thermal stability of the IL-ZnO composite materials is sustained by the electrostatic repulsion between the nanoparticles. The cationic components of the IL are bound to the ZnO NC cores through the carboxylate moieties (see Supporting Information), and the positive charges of the cationic species are balanced by the $[N(Tf)_2]^-$ counterions. The ZnO NCs protected by the positively charged species and separated by the counterions are not able to come into contact with one another, even after thermal treatment, to form aggregates or to undergo Ostwald ripening because of this electrostatic repulsion (see the schemes in the Supporting Information).

In conclusion, we have demonstrated a new route for the stabilization of ZnO NCs that show tunable photoluminescence. Their excellent photoluminescence, high thermal stability, and good processability in both the solvated and solvent-free state make these composites highly applicable as new luminescent materials.

Experimental Section

Zinc bromoacetate: Excess $Zn(OH)_2$, which was freshly precipitated from an aqueous solution of $ZnCl_2$ by addition of NaOH, was mixed with an aqueous solution of 10 mmol of bromoacetic acid and the mixture was heated at 70 °C with vigorous stirring until the pH value of the system reached about 6.0. The residual $Zn(OH)_2$ was then removed by filtration and the filtrate was concentrated on a rotary evaporator. The resulting solid was dried in a vacuum oven at 100 °C.

N,*N*-dimethyloctadecylammonium bromide acetate zinc salt (C_{18}-Zn): *N*,*N*-dimethyloctadecylamine (Aldrich; 10 mmol) and zinc bromoacetate (5 mmol) were dissolved in absolute ethanol (50 mL) and the vigorously stirred solution was heated under reflux for 24 h in a 100-mL round-bottomed flask. The solution was then concentrated on a rotary evaporator to about 4 mL. This solution was cooled to −12 °C and anhydrous diethyl ether (20 mL) was added to precipitate C_{18}-Zn as a white solid (3 mmol, 2.81 g), which was isolated by filtration and washed with anhydrous diethyl ether. To remove the residual zinc bromoacetate from the product completely, the solid was redissolved in chloroform, filtered, and dried by evaporation. ^{1}H NMR ($CDCl_3$, TMS): $\delta = 4.15$ (s, 2H), 3.59 (t, $J = 7.0$ Hz, 2H), 3.35 (s, 6H), 1.72 (s, 2H), 1.33–1.28 (m, 6H), 1.26 (s, 24H), 0.89 ppm (t, $J = 7.0$ Hz, 3H).

N,N-dimethyloctadecylammonium bis((trifluoromethyl)sulfonyl)amide acetate zinc salt (IL-Zn): An aqueous solution (50 mL) of C_{18}-Zn (1 mmol) and an aqueous solution (50 mL) of lithium bis((trifluoromethyl)sulfonyl)amide ($LiN(Tf)_2$) (Fluka, 2 mmol) were mixed and heated at 70 °C for several minutes whilst stirring until the solution turned turbid. Chloroform (50 mL) was then added to the hot mixture to extract the reaction product. The extract was concentrated on a rotary evaporator and dried in vacuo at 70 °C to give 0.97 mmol of IL-Zn.

IL-ZnO: IL-Zn (1 mmol) was treated with LiOH in ethanol at room temperature. The [LiOH]/[Zn] molar ratio in the reaction system was controlled to be 3.5, 1.4, and 1.0, respectively for IL-ZnO-A, -B, -C. The resulting solution was evaporated to dryness on a rotary evaporator and the obtained solid product was re-dissolved in 20 mL of chloroform to form a stable 0.02 M colloidal solution.

Characterization: ^{1}H NMR spectra (with tetramethylsilane as reference) were recorded with a Bruker Ultrashield 500 MHz NMR spectrometer and the IR spectra were recorded with a Bruker IFS 66v/S FTIR spectrometer equipped with a DGTS detector. A Perkin–Elmer LS 55 luminescence spectrometer was used to obtain the photoluminescence spectra for the IL-ZnO materials both in their solvated and solvent-free states. The HRTEM images were recorded with a JEOL JEM-3010 transmission electron microscope operating at 300 kV. The thermogravimetric and differential thermal analysis (TG-DTA) curves were recorded with a Perkin–Elmer Pyris Diamond TG/DTA thermal analyzer at a temperature-increase rate of 20 °C min^{-1} under nitrogen. The DSC measurements were performed with a Netzsch DSC 204 calorimeter at a scanning rate of 10 °C min^{-1}.

For evaluation of the fluorescence QYs of the IL-ZnO materials, quinine sulfate in 0.5 M sulfuric acid was used as the reference for the sample emitting blue light while rhodamine 6G in ethanol was used for those emitting green and yellow light.[7]

Received: June 16, 2006

Keywords: ionic liquids · nanocrystals · photoluminescence · quantum yield · zinc

---

[1] a) V. L. Colvin, M. C. Schlamp, A. P. Alivisatos, *Nature* **1994**, *370*, 354; b) W. C. W. Chan, S. Nie, *Science* **1998**, *281*, 2016; c) S. Coe, W. K. Woo, M. Bawendi, V. Bulovic, *Nature* **2002**, *420*, 800.

[2] a) A. P. Alivisatos, *Science* **1996**, *271*, 933; b) B. O. Dabbousi, J. Rodriguez-Viejo, F. V. Mikulec, J. R. Heine, H. Mattoussi, R. Ober, K. F. Jensen, M. G. Bawendi, *J. Phys. Chem. B* **1997**, *101*, 9463; c) A. Pan, H. Yang, R. Liu, R. Yu, B. Zou, Z. Wang, *J. Am. Chem. Soc.* **2005**, *127*, 15692.

[3] a) L. Qu, Z. Peng, X. Peng, *Nano Lett.* **2001**, *1*, 333; b) X. Zhong, R. Xie, Y. Zhang, T. Basché, W. Knoll, *Chem. Mater.* **2005**, *17*, 4038.

[4] a) L. Spanhel, M. Haase, H. Weller, A. Henglein, *J. Am. Chem. Soc.* **1987**, *109*, 5649; b) C. B. Murray, D. J. Norris, M. G. Bawendi, *J. Am. Chem. Soc.* **1993**, *115*, 8706; c) M. A. Hines, P. Guyot-Sionnest, *J. Phys. Chem. B* **1998**, *102*, 3655; d) J. S. Steckel, J. P. Zimmer, S. Coe-Sullivan, N. E. Stott, V. Bulović, M. G. Bawendi, *Angew. Chem.* **2004**, *116*, 2206; *Angew. Chem. Int. Ed.* **2004**, *43*, 2154.

[5] W. Z. Ostwald, *Phys. Chem.* **1901**, *37*, 385.

[6] A. Henglein, *Chem. Rev.* **1989**, *89*, 1861.

[7] H. M. Xiong, D. P. Liu, Y. Y. Xia, J. S. Chen, *Chem. Mater.* **2005**, *17*, 3062.

[8] H. M. Xiong, Z. D. Wang, Y. Y. Xia, *Adv. Mater.* **2006**, *18*, 748.

[9] D. G. Kurth, P. Lehmann, C. Lesser, *Chem. Commun.* **2000**, 949.

[10] a) H. Zhang, Z. Cui, Y. Wang, K. Zhang, X. Ji, C. Lü, B. Yang, M. Gao, *Adv. Mater.* **2003**, *15*, 777; b) H. Zhang, C. Wang, M. Li, J. Zhang, G. Lu, B. Yang, *Adv. Mater.* **2005**, *17*, 853.

[11] a) T. Nakashima, T. Kawai, *Chem. Commun.* **2005**, 1643; b) T. Nakashima, T. Sakakibara, T. Kawai, *Chem. Lett.* **2005**, *34*, 1410.

[12] a) V. Mévellec, B. Leger, M. Mauduit, A. Roucoux, *Chem. Commun.* **2005**, 2838; b) M. Antonietti, D. Kuang, B. Smarsly, Y. Zhou, *Angew. Chem.* **2004**, *116*, 5096; *Angew. Chem. Int. Ed.* **2004**, *43*, 4988; c) J. Dupont, G. S. Fonseca, A. P. Umpierre, P. F. P. Fichtner, S. R. Teixeira, *J. Am. Chem. Soc.* **2002**, *124*, 4228.

[13] a) A. B. Bourlinos, R. Herrera, N. Chalkias, D. D. Jiang, Q. Zhang, L. A. Archer, E. P. Giannelis, *Adv. Mater.* **2005**, *17*, 234; b) A. B. Bourlinos, A. Stassinopoulos, D. Anglos, R. Herrera, S. H. Anastasiadis, D. Petridis, E. P. Giannelis, *Small* **2006**, *2*, 513.

[14] P. Wasserscheid, W. Keim, *Angew. Chem.* **2000**, *112*, 3926; *Angew. Chem. Int. Ed.* **2000**, *39*, 3772.

[15] A. Wood, M. Giersig, M. Hilgendorff, A. Vilas-Campos, L. M. Liz-Marzán, P. Mulvaney, *Aust. J. Chem.* **2003**, *56*, 1051.

[16] a) K. Vanheusden, W. L. Warren, J. A. Voigt, C. H. Seager, D. R. Tallant, *Appl. Phys. Lett.* **1995**, *67*, 1280; b) K. Vanheusden, W. L. Warren, C. H. Seager, D. R. Tallant, J. A. Voigt, B. E. Gnade, *J. Appl. Phys.* **1996**, *79*, 7983; c) A. van Dijken, E. A. Meulenkamp, D. Vanmaekelbergh, A. Meijerink, *J. Phys. Chem. B* **2000**, *104*, 1715.

[17] A. van Dijken, J. Makkinje, A. Meijerink, *J. Lumin.* **2001**, *32*, 323.